## Title

Dynamic contrast-enhanced (DCE) MR imaging: the role of qualitative and quantitative parameters for evaluating prostate tumors stratified by Gleason score and PI-RADS v2



## Journal

Abdominal Radiology, 45(7)

## ISSN

2366-004X

## Authors

Afshari Mirak, Sohrab
Mohammadian Bajgiran, Amirhossein
Sung, Kyunghyun
et al.

## Publication Date

2020-07-01

## DOI

10.1007/s00261-019-02234-6

Peer reviewed

HHS Public Access

Author manuscript

*Abdom Radiol (NY)*. Author manuscript; available in PMC 2023 June 13.

Published in final edited form as:

*Abdom Radiol (NY)*. 2020 July ; 45(7): 2225–2234. doi:10.1007/s00261-019-02234-6.

# Dynamic contrast-enhanced (DCE) MR imaging: the role of qualitative and quantitative parameters for evaluating prostate tumors stratified by Gleason score and PI-RADS v2

**Sohrab Afshari Mirak**[1], **Amirhossein Mohammadian Bajgiran**[1], **Kyunghyun Sung**[1], **Nazanin H. Asvadi**[1], **Daniela Markovic**[1], **Ely R. Felker**[1], **David Lu**[1], **Anthony Sisk**[2], **Robert E. Reiter**[3], **Steven S. Raman**[1,3]

[1]Department of Radiological Sciences, David Geffen School of Medicine at UCLA, 757 Westwood Plaza, Los Angeles, CA 90095, USA

[2]Department of Pathology, David Geffen School of Medicine at UCLA, 10833 Le Conte Ave, AS-370 CHS, Los Angeles, CA 90095, USA

[3]Department of Urology, David Geffen School of Medicine at UCLA, Clark Urology Center – Westwood, 200 UCLA Medical Plaza, Suite 140, Los Angeles, CA 90095, USA

## Abstract

**Purpose—**To investigate the role of qualitative and quantitative DCE-MRI parameters in prostate cancer (PCa) stratified by whole-mount histopathology (WMHP) Gleason score (GS) and PI-RADSv2.

**Methods—**This retrospective study included 323 PCa tumors in 254 men, who underwent 3T MRI prior to prostatectomy, 7/2009–12/2016. Qualitative DCE curve types included type 1 (progressive), type 2 (plateau) and type 3 (washout). Quantitative DCE-MRI pharmacokinetic (PK) parameters included $K^{trans}$ (influx volume transfer coefficient), $K_{ep}$ (efflux reflux rate constant) and iAUC (initial area under the curve). DCE-MRI features of true positive lesions were evaluated for overall, index, transition zone (TZ) and peripheral zone (PZ), based on GS grade (low = 6, high > 6) and PI-RADSv2 score using SPSSv24.

**Results—**There were 57 (17.6%) low-grade and 266 (82.4%) high-grade PCa lesions. PI-RADSv2 3, 4 and 5 included 106, 120 and 97 lesions, respectively. 251 (77.7%) and 72 (22.3%) lesions were located in PZ and TZ, respectively. High-grade lesions had significantly higher proportion of Type 3 curves compared to low-grade lesions in overall (70.3% vs. 54.4%) and TZ (73.5% vs. 43.5%). As PI-RADSv2 increased, the proportion of type 3 curve significantly increased for overall (80.4–51.9%), index (80.4–54.7%) and PZ (78.7–52.1%) lesions. Among PK parameters, $K^{trans}$ (0.43 vs 0.32) and iAUC (8.99 vs 6.9) for overall PCa, $K^{trans}$ (0.43 vs 0.31)

✉Sohrab Afshari Mirak, safsharimirak@mednet.ucla.edu.

**Electronic supplementary material** The online version of this article (https://doi.org/10.1007/s00261-019-02234-6) contains supplementary material, which is available to authorized users.

Compliance with ethical standards

**Ethical approval** This study was performed in accordance with the 1996 Health Information Portability and Accountability Act (HIPAA) and under waiver of informed consent by the institutional review board (IRB).

and iAUC (9 vs 6.67) for PZ PCa, and iAUC (8.94 vs 7.42) for index PCa were significantly higher for high-grade versus low-grade lesions. Also, $K^{trans}$ (0.51–0.34), $K_{ep}$ (1.75–1.29) and iAUC (9.79–7.6) for overall PCa, $K^{trans}$ (0.53–0.32), $K_{ep}$ (1.81–1.26) and iAUC (9.83–7.34) for PZ PCa; and $K_{ep}$ (1.79–1.17) and iAUC (11.3–8.45) for index PCa increased significantly with a higher PI-RADSv2 score.

**Conclusions—**The results of study show the possible utility of qualitative and quantitative DCE-MRI parameters for assessment of PCa GS and PI-RADSv2 categorization.

### Keywords

Prostate cancer; Magnetic resonance imaging; Perfusion imaging; Prostate Imaging and Reporting Data System

## Introduction

Dynamic contrast-enhanced (DCE) magnetic resonance imaging (MRI) is a technique that provides both morphologic and functional tissue information from qualitative and quantitative analysis of dynamic and static tissue enhancement characteristics after intravenous injection of gadolinium-based extracellular contrast [1]. Angiogenesis and neovascularization are the main characteristics of cellular growth, caused by a cascade of stimulating factors, mainly the vascular endothelial growth factor [2–4]. However, the endothelial lining of these neoangiogenic vessels is inherently more permeable leading to leakage of intravenous gadolinium-based agents into the surrounding tissue [4, 5]. On DCE MRI, many types of malignancies including prostate cancer (PCa) lesions tend to enhance and de-enhance earlier than surrounding normal tissue due in part to these properties [6, 7].

The Prostate Imaging–Reporting and Data System version 2 (PI-RADSv2) scoring system recognizes the value of DCE MRI as an imaging biomarker to improve PCa detection; however, the performance of DCE MRI in PI-RADSv2 is limited to visual assessment of early and focal enhancement of the targets as compared to the surrounding tissue in peripheral zone lesions, and no detailed information is considered for the categorization of the lesions [8]. Prior studies have reported variable results regarding the utility of different DCE MRI qualitative and quantitative parameters in detection of PCa [9, 10] especially when stratified by zonal anatomy [transition zone (TZ) vs peripheral zone (PZ)]. It also has a recognized role in tumor staging (capsular penetration and seminal vesicle invasion) and detection of suspected tumor recurrence following surgical and nonsurgical treatment [2]. However, the potential uses for individual DCE MRI parameters such as the qualitative enhancement curve types and the quantitative pharmacokinetic (PK) parameters and their ability to discriminate low- from high-grade PCa as well as the correlation of these parameters with the standard PCa scoring categories have been incompletely studied.

The purpose of this study was to critically evaluate the performance of individual qualitative and quantitative DCE-MRI parameters on 3T multiparametric MRI (3T mpMRI) for evaluating PCa in low-grade and high-grade lesions as well as different PI-RADSv2 categories using whole mount histopathology (WMHP) as the reference standard.

## Materials and methods

### Patientsalonzi

This study was conducted in compliance with 1996 Health Insurance Portability and Accountability Act (HIPAA) and approved by the Institutional Review Board (IRB) with waiver of requirement for informed consent. The study cohort was derived from our database of 531 consecutive men with 1039 PCa lesions, who underwent 3T mpMRI within 6 months prior to robotic assisted radical prostatectomy at a single, high-volume tertiary care academic center between June 2009 and December 2016 (Fig. 1). 3T mpMRI was performed in patients with clinically suspected PCa for the following reasons: elevated PSA, elevated PSA density or PSA velocity for either targeted biopsy planning and/or surgical staging. The true positive lesions were included in the study, while the patients with prior radiotherapy, partial prostate resection and those with technical limitations were excluded from the study, which resulted in a study population of 254 patients with 323 PCa lesions [mean age: 62.1 ± 7.6 (41–80) years] (Fig. 1).

### MRI technique

All men in this cohort underwent preoperative mpMRI using one of the three available 3 Tesla scanners [Siemens Magnetom Trio, Skyra or Verio scanners (Siemens Medical Systems, Malvern, Pennsylvania, USA)] with pelvic external phased array coil with or without an endorectal coil (MEDRAD, Indianola, PA., USA) using nearly identical imaging protocols based on the PI-RADSv2 criteria. Patients were given 1 mg of an anti-peristaltic agent [glucagon (GlucaGen, Lilly, In, USA)] intramuscularly to reduce bowel peristalsis.

The 3T MRI protocol is described in Table 1. For the DCE imaging, a dynamic view-sharing time-resolved angiography with stochastic trajectories gradient-echo T1-weighted sequence was performed over 6 min (4.75 s per acquisition) with a 15 s injection delay (TWIST, Siemens Healthineers, Malvern PA) after intravenous injection of 0.1 mg/kg Gadobenate Dimeglumine (MultiHance, Bracco) at 2 cc/s at the second acquisition for baseline calculation. PI-RADSv2 defined qualitative DCE curve types for each enhancing region of interest (ROI) included type 1 (progressive enhancement), type 2 (plateau) and type 3 (washout).

### Image analysis

3T mpMRI interpretation was performed by an abdominal imaging fellow and one of three board-certified abdominal radiologists with 3–18 years of experience in developing and interpreting prostate MRI using commercially available third party software on a networked workstation (DynaCAD; In vivo, Gainesville, FL). Quantitative DCE-MRI was computed by a standard Parker two-compartment PK model [11]. Quantitative PK values analysis included the following: $K^{trans}$ (influx volume transfer coefficient), $K_{ep}$ (efflux reflux rate constant) and iAUC (initial area under the curve)). Each radiologist outlined suspicious foci primarily on the DWI sequences in the PZ or T2-weighted imaging (T2WI) sequences in the TZ and outlined and scored suspicious regions of interest (ROI) based on PI-RADSv2, assigning each ROI a score on a 5 point scale for suspected PCa (1—least suspicious, 5—most suspicious). Besides PIRADS score, the standard ROI for the most suspicious area of

the tumor was used for the evaluation of lesion's other characteristics, including lesion size which was measured in the image with the largest diameter in the axial plane (Fig. 2). The measurements were consistent between all readers. As a part of clinical workflow, the MR images were evaluated prospectively and the information was gathered retrospectively from the original reports. The radiologists were blinded to the exact indication of MRI (either diagnosis or staging) at the time of interpretation and the final diagnosis was made based on some clinical information when available. PI-RADSv2 was assigned prospectively for cases after 2015 and retrospectively for cases before 2015 (with the radiologist being blinded to the patients' clinical and biopsy results). PZ PCa lesions, which were upgraded from PI-RADSv2 score 3 to 4 based on DCE findings, were downgraded to score 3 to evaluate the DCE parameters individually in each category.

## Reference standard

The resected prostate specimens were embedded in paraffin and sectioned in the axial plane from the inked basal margin to the apex in approximately 5 mm intervals. The sections were cut at 4 microns, stained with Hematoxylin and Eosin in an automatic stainer (Tissue Tech Prisma Plus), and mounted on large slides for WMHP analysis by two genitourinary pathologists with 4–12 years of experience in interpreting prostates. Each PCa tumor was localized, measured and outlined while characteristics such as location (using PI-RADSv2 sector mapping) and Gleason score (GS) were also noted. At a monthly separate joint meeting ("match meeting"), a genitourinary radiologist and a genitourinary pathologist reviewed each case individually to match 3T mpMRI ROIs to the corresponding locations on the previously reported WMHP. Lesions were deemed true positive if they were in the same quadrant (left, right, anterior and posterior) and in the appropriate segment (base, midgland and apex) on both 3T mpMRI and WMHP. Each WMHP slide was photographed at × 10 and × 100, and each whole mount slide was scanned for inclusion in our database. Index lesion was defined as the lesion with the highest GS and as the one with the largest diameter if the GS is same for several tumors.

Each patient's age, PSA level, MRI (PI-RADSv2 scoring, enhancement curve type and pharmacokinetic parameters), and histopathological (location (TZ vs PZ) and GS) information was gathered through patient charts, compliant with patient confidentiality. All information was entered into our database. PSA density was measured by deviding PSA level to prostate volume.

## Statistical analysis

Statistical analysis was performed using SPSS software version 24 (Chicago, Ill, USA). All true positive PCa lesions were evaluated. Continuous variables were expressed using median and Interquartile Range (IQR) and categorical values were reported as frequencies and percentages. DCE MRI qualitative and quantitative parameters were compared across lesions between low-grade and high-grade PCa lesions (low = 6, high > 6), different PI-RADSv2 scores and based on International Society of Urological Pathology (ISUP) grading classifications (Supplementary Table 1) using logistic and linear regression models, respectively allowing for random person effects to account for the fact that observations within the same patient were not independent. The assessments were done for overall and

index PCa lesions as well as based on lesion location (TZ and PZ) and size (< 1 cm and ≥ 1 cm), individually. Level of statistical significance was considered as $p < 0.05$.

The accuracies of DCE parameters for predicting tumor grading were assessed using receiver operating characteristic curve (ROC) analysis. The ROC analysis was performed under random effects logistic regression models including the following 7 models: (1) curve type, (2) ADC, (3) $K^{trans}$, (4) $K_{ep}$, (5) iAUC, (6) PI-RADSv2 and (7) PI-RADSv2 (DWI score for PZ and PI-RADSv2 score for TZ) + $K^{trans}$ + $K_{ep}$ + iAUC + curve type. Specifically, we hypothesized that the DCE qualitative and quantitative parameters ($K^{trans}$ $K_{ep}$, iAUC and curve type) would improve the prediction of tumor grading beyond PI-RADSv2 alone. We formally tested this hypothesis by comparing the areas under the ROC curve for models 7 versus 6 above.

## Results

Table 2 shows clinical, 3T mpMRI and pathological characteristics of the lesions.

In Tables 3 and 4, the qualitative (enhancement curve types 1–3) and quantitative ($K^{trans}$, $K_{ep}$, and iAUC) DCE MRI parameters for PCa lesions are shown with comparison of the results between low- and high-grade lesions as well as different PI-RADSv2 scores for overall and index PCa lesions stratified by tumor size and zonal location. Overall and TZ high-grade PCa lesions had significantly higher proportion of Type 3 curves and lower proportion of Type 2 curves as compared to low-grade PCa lesions. For true positive ROI lesions, higher PI-RADSv2 scores had significantly higher proportion of lesions with type 3 curves and lower proportion of lesions with type 2 curves for overall, index, PZ and ≥ 1 cm lesions, with a trend to significance in TZ lesions. Figure 3 and 4 show ROIs contoured on 3T mpMRI sections with corresponding WMHP sections in two patients; with curve types 2 in a low-grade PCa lesion and curve type 3 in a high-grade PCa lesion, respectively. Among PK parameters, $K^{trans}$ and iAUC for overall, PZ and ≥ 1 cm; and iAUC for index PCa lesions were significantly higher in high grade as compared to low-grade lesions. Also, $K^{trans}$, $K_{ep}$ and iAUC for overall, PZ and ≥ 1 cm PCa lesions; and $K_{ep}$ and iAUC in index PCa lesions significantly increased with higher level of suspicion for malignancy using PI-RADSv2 scoring.

The results of the ROC curves for differentiating high-grade from low-grade PCa showed significantly higher performance of PI-RADSv2 (AUC 0.73) as compared to ADC (AUC 0.68), iAUC (AUC 0.65), $K^{trans}$ (AUC 0.64), $K_{ep}$ (AUC 0.60) and curve type (AUC 0.58) (overall $p$ value 0.02). Besides, the combination of qualitative and quantitative DCE parameters and PI-RADSv2 category showed significantly higher performance for tumor grading as compared to PI-RADSv2 alone (AUC; 0.78 vs 0.73) ($p$ value 0.0084) (Fig. 5).

## Discussion

In this study with WMHP correlation, we demonstrated that overall, index, PZ, and larger lesions with high PI-RADSv2 score in 3T mpMRI and overall and PZ PCa with high Gleason scores are associated with significantly higher proportion of qualitative DCE-MRI curve type 3 compared to types 1 and 2. We also demonstrated that DCE derived quantitative

PK parameters were significantly greater in MRI derived ROIs with high PI-RADSv2 scores for overall ($K^{trans}$, $K_{ep}$ and iAUC), index ($K_{ep}$ and iAUC), PZ ($K^{trans}$, $K_{ep}$ and iAUC) and larger ($K^{trans}$, $K_{ep}$ and iAUC) PCa lesions as well as in high pathology Gleason grade (≥7) for overall ($K^{trans}$, iAUC), index (iAUC), PZ ($K^{trans}$, iAUC) and larger ($K^{trans}$, iAUC) PCa lesions. Also, the results of this study showed better performance of PI-RADSv2 when combined with DCE qualitative and quantitative parameters for PCa grading.

Currently, the therapeutic decision for patients with PCa is based on the surrogate markers for assessing PCa volume and aggressiveness, which have historically been derived from PSA measurement and results of invasive techniques such as transrectal ultrasound (TRUS) template biopsy. Using noninvasive techniques for defining the aggressiveness of the tumors will result in lower complications and biopsy will be reserved for selective patients with equivocal imaging outcomes or incompatible clinical manifestations [12]. In patients undergoing robotic assisted radical prostatectomy, 3T mpMRI imaging has been shown to detect 47% of all PCa lesions and 72% of clinically significant PCa [13]. PI-RADSv2 based targets on 3T mpMRI have been shown to be effective for risk stratification of patients who undergo 3T MR-guided biopsy [14]. DCE-MRI has been demonstrated to be more robust than T2WI for localization of PCa lesions [15]. DCE qualitative type 2 and type 3 enhancement curve types are associated with a higher chance of malignancy. However, quantitative and semi quantitative DCE MRI parameters have shown higher performance for differentiating normal from cancerous tissue, especially in the PZ [16]. Although a number of studies have suggested to perform MRI without contrast as it provides similar PCa detection rates compared to mpMRI with contrast [17, 18], several prior studies have generally shown that DCE was correlated with PCa aggressiveness. In the study of 34 patients with biopsy correlation using 1.5 Tesla MRI, Futterer et al. reported the initial utility of DCE for PCa localization [15]. In another study including 45 prostatectomy patients using 3 Tesla MRI, Vos et al. reported that quantitative and semi quantitative DCE parameters had the potential to assess PCa aggressiveness in the PZ and also among these parameters, wash-in, $K^{trans}$, and $K_{ep}$ offer the best possibility to discriminate low-, intermediate-, and high-grade PCa lesions [5]. In a study of 43 patients with prostatectomy correlation using 3 Tesla MRI, Rosenkrantz et al. reported that although the use of a semiquantitative or quantitative model for detection of PZ PCa lesion provides greater sensitivity compared with a qualitative model for an experienced reader, none of the perfusion models were associated with higher GS [7]. In a study of 48 patients with prostatectomy correlation using 3 Tesla MRI, Peng et al. reported that $K^{trans}$ values correlated with tumor GS [19]. In a similar study with 36 PCa patients, Sanz-Requena et al. concluded that the normalized $K^{trans}$, upslope, and AUC60 have good diagnostic accuracy to characterize tumor aggressiveness [9]. Using 1.5 Tesla MRI with biopsy correlation in a study of 43 patients, Chen et al. reported that washout gradient is a potential marker for GS and has a good diagnostic performance in assessing tumor aggressiveness [20]. The present study with a larger sample size, in part is consistent with previous findings. Our results showed that high-grade tumors had a significantly higher rate of the type 3 curve, while low-grade tumors had a significantly higher rate of the type 2, in overall and TZ lesions. Besides, median $K^{trans}$, $K_{ep}$, and iAUC in the overall, PZ, and larger PCa lesions and median iAUC in index lesions were significantly higher in high-grade compared to low-grade PCa

lesions. The higher performance of PK parameters of DCE MRI for tumor aggressiveness in PZ and larger lesions as compared to TZ and smaller lesions can be partially explained by the possible similar enhancement behavior of the structures such as benign prostatic hyperplasia in TZ as well as the small number of the samples in these two subgroups. Although the results of the study showed higher performance of PI-RADSv2 scoring system for PCa grading, it suggests even higher utility when combining qualitative and quantitative DCE parameters with PI-RADSv2 after removing the effect of DCE positivity on upgrading the PZ lesions from category 3–4.

Different methods have been introduced to improve DCE MRI analysis, some of which have focused on simplifying the interpretation [21]. Use of computer-aided diagnosis has also been applied to achieve reliable prostate tissue characterization in an automated and presumably more reproducible fashion [16, 19]. However, DCE has some limitations, including use of gadolinium chelates, increased MRI time, cumbersome nature of quantitative image interpretation, and post-processing and variable utility. [7, 22] The aforementioned limitations and a lack of uniformity in its interpretation have rendered it as a secondary qualitative image interpretation tool in PI-RADSv2. The results of our study showed significantly higher number of curve type 3 in lesions with higher PI-RADSv2 scores (4&5) for overall, index, PZ, and larger PCa lesions. However, $K^{trans}$, $K_{ep}$, and iAUC in overall, PZ, and larger PCa lesions and $K_{ep}$ and iAUC in index PCa lesions were significantly higher in higher PI-RADS scores (4&5) compared to lower scores (3). This suggests high utility of various DCE MRI qualitative and quantitative parameters for scoring PCa lesions.

There are some limitations to the study. The patients were selected from a tertiary referral center with subspeciality expertise in urological oncology. The study was conducted in patients who underwent prostatectomy, with exclusion of patients with other treatment modalities. These may impose limitations in the generalization of the results of the study. Due to the retrospective nature of the study, a significant number of patients were excluded because of missed DCE parameters, however, the study population included a significant number of patients, which will minimize the selection bias. Also, as the patients were selected from our resection database, there was no information provided regarding the number of cases being scanned in each scanner; however, the imaging protocols were nearly identical between the scanners and met the criteria for PI-RADSv2. All lesions were evaluated by a single radiologist as a part of clinical workflow and the data was gathered retrospectively from the original reports. As a result, the intra- and inter-reader variability for the lesion scoring and measurements were not evaluated in this study.

In conclusion, the present study found that more aggressive DCE qualitative and quantitative parameters correlate with PCa aggressiveness features in imaging and pathology. However, it seems that these parameters may be more utilized in overall, PZ, and larger PCa lesions and in combination with PI-RADSv2 category. The results of this study can suggest that DCE can be an adjuct to DWI and T2WI sequences in the discrimination of more aggressive PCa.

## Supplementary Material

Refer to Web version on PubMed Central for supplementary material.

## Acknowledgements

This work was supported by funds from the Integrated Diagnostics Program, Department of Radiological Sciences & Department of Pathology and Laboratory Medicine in our institution. We are grateful to Dr. Melina Hosseini and Dr. Sepideh Shakeri for editing the final version of the manuscript.

## References

1. Isebaert S, De Keyzer F, Haustermans K, Lerut E, Roskams T, Roebben I, Van Poppel H, Joniau S, Oyen R (2012) Evaluation of semi-quantitative dynamic contrast-enhanced MRI parameters for prostate cancer in correlation to whole-mount histopathology. Eur J Radiol 81 (3):e217–222. doi:10.1016/j.ejrad.2011.01.107 [PubMed: 21349667]
2. Alonzi R, Padhani AR, Allen C (2007) Dynamic contrast enhanced MRI in prostate cancer. Eur J Radiol 63 (3):335–350. doi:10.1016/j.ejrad.2007.06.028 [PubMed: 17689907]
3. Bonekamp D, Jacobs MA, El-Khouli R, Stoianovici D, Macura KJ (2011) Advancements in MR imaging of the prostate: from diagnosis to interventions. Radiographics 31 (3):677–703. doi:10.1148/rg.313105139 [PubMed: 21571651]
4. Kuhl CK, Schild HH (2000) Dynamic image interpretation of MRI of the breast. J Magn Reson Imaging 12 (6):965–974 [PubMed: 11105038]
5. Vos EK, Litjens GJ, Kobus T, Hambrock T, Hulsbergen-van de Kaa CA, Barentsz JO, Huisman HJ, Scheenen TW (2013) Assessment of prostate cancer aggressiveness using dynamic contrast-enhanced magnetic resonance imaging at 3 T. Eur Urol 64 (3):448–455. doi:10.1016/j.eururo.2013.05.045 [PubMed: 23751135]
6. Girouin N, Mege-Lechevallier F, Tonina Senes A, Bissery A, Rabilloud M, Marechal JM, Colombel M, Lyonnet D, Rouviere O (2007) Prostate dynamic contrast-enhanced MRI with simple visual diagnostic criteria: is it reasonable? Eur Radiol 17 (6):1498–1509. doi:10.1007/s00330-006-0478-9 [PubMed: 17131126]
7. Rosenkrantz AB, Sabach A, Babb JS, Matza BW, Taneja SS, Deng FM (2013) Prostate cancer: comparison of dynamic contrast-enhanced MRI techniques for localization of peripheral zone tumor. AJR Am J Roentgenol 201 (3):W471–478. doi:10.2214/ajr.12.9737 [PubMed: 23971479]
8. Radiology ACo (2014) PIRADS v2. Reston, Va: American College of Radiology
9. Sanz-Requena R, Marti-Bonmati L, Perez-Martinez R, Garcia-Marti G (2016) Dynamic contrast-enhanced case-control analysis in 3T MRI of prostate cancer can help to characterize tumor aggressiveness. Eur J Radiol 85 (11):2119–2126. doi:10.1016/j.ejrad.2016.09.022 [PubMed: 27776667]
10. Noworolski SM, Henry RG, Vigneron DB, Kurhanewicz J (2005) Dynamic contrast-enhanced MRI in normal and abnormal prostate tissues as defined by biopsy, MRI, and 3D MRSI. Magn Reson Med 53 (2):249–255. doi:10.1002/mrm.20374 [PubMed: 15678552]
11. Tofts PS (1997) Modeling tracer kinetics in dynamic Gd-DTPA MR imaging. J Magn Reson Imaging 7 (1):91–101 [PubMed: 9039598]
12. Hara N, Okuizumi M, Koike H, Kawaguchi M, Bilim V (2005) Dynamic contrast-enhanced magnetic resonance imaging (DCE-MRI) is a useful modality for the precise detection and staging of early prostate cancer. Prostate 62 (2):140–147. doi:10.1002/pros.20124 [PubMed: 15389803]
13. Le JD, Tan N, Shkolyar E, Lu DY, Kwan L, Marks LS, Huang J, Margolis DJ, Raman SS, Reiter RE (2015) Multifocality and prostate cancer detection by multiparametric magnetic resonance imaging: correlation with whole-mount histopathology. Eur Urol 67 (3):569–576. doi:10.1016/j.eururo.2014.08.079 [PubMed: 25257029]
14. Tan N, Lin WC, Khoshnoodi P, Asvadi NH, Yoshida J, Margolis DJ, Lu DS, Wu H, Sung KH, Lu DY, Huang J, Raman SS (2017) In-Bore 3-T MR-guided Transrectal Targeted Prostate Biopsy: Prostate Imaging Reporting and Data System Version 2-based Diagnostic Performance

for Detection of Prostate Cancer. Radiology 283 (1):130–139. doi:10.1148/radiol.2016152827 [PubMed: 27861110]

15. Futterer JJ, Heijmink SW, Scheenen TW, Veltman J, Huisman HJ, Vos P, Hulsbergen-Van de Kaa CA, Witjes JA, Krabbe PF, Heerschap A, Barentsz JO (2006) Prostate cancer localization with dynamic contrast-enhanced MR imaging and proton MR spectroscopic imaging. Radiology 241 (2):449–458. doi:10.1148/radiol.2412051866 [PubMed: 16966484]
16. Scheenen TW, Rosenkrantz AB, Haider MA, Futterer JJ (2015) Multiparametric Magnetic Resonance Imaging in Prostate Cancer Management: Current Status and Future Perspectives. Invest Radiol 50 (9):594–600. doi:10.1097/rli.0000000000000163 [PubMed: 25974203]
17. Mussi TC, Martins T, Garcia RG, Filippi RZ, Lemos GC, Baroni RH (2017) Are Dynamic Contrast-Enhanced Images Necessary for Prostate Cancer Detection on Multiparametric Magnetic Resonance Imaging? Clin Genitourin Cancer 15 (3):e447–e454. doi:10.1016/j.clgc.2016.10.001 [PubMed: 27856204]
18. Scialpi M, Rondoni V, Aisa MC, Martorana E, D'Andrea A, Malaspina CM, Orlandi A, Galassi G, Orlandi E, Scialpi P, Dragone M, Palladino D, Simeone A, Amenta M, Bianchi G (2017) Is contrast enhancement needed for diagnostic prostate MRI? Transl Androl Urol 6 (3):499–509. doi:10.21037/tau.2017.05.31 [PubMed: 28725592]
19. Peng Y, Jiang Y, Yang C, Brown JB, Antic T, Sethi I, Schmid-Tannwald C, Giger ML, Eggener SE, Oto A (2013) Quantitative analysis of multiparametric prostate MR images: differentiation between prostate cancer and normal tissue and correlation with Gleason score--a computer-aided diagnosis development study. Radiology 267 (3):787–796. doi:10.1148/radiol.13121454 [PubMed: 23392430]
20. Chen YJ, Chu WC, Pu YS, Chueh SC, Shun CT, Tseng WY (2012) Washout gradient in dynamic contrast-enhanced MRI is associated with tumor aggressiveness of prostate cancer. J Magn Reson Imaging 36 (4):912–919. doi:10.1002/jmri.23723 [PubMed: 22711415]
21. Haq NF, Kozlowski P, Jones EC, Chang SD, Goldenberg SL, Moradi M (2015) A data-driven approach to prostate cancer detection from dynamic contrast enhanced MRI. Comput Med Imaging Graph 41:37–45. doi:10.1016/j.compmedimag.2014.06.017 [PubMed: 25060941]
22. Quon J, Kielar AZ, Jain R, Schieda N (2015) Assessing the utilization of functional imaging in multiparametric prostate MRI in routine clinical practice. Clin Radiol 70 (4):373–378. doi:10.1016/j.crad.2014.12.001 [PubMed: 25578231]

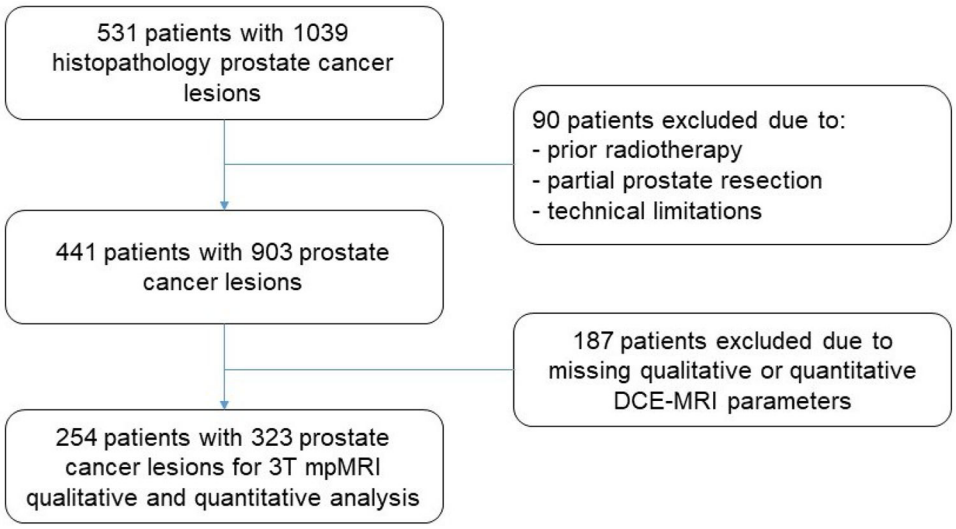


**Fig. 1.**
Flow diagram shows patient selection used for this retrospective study

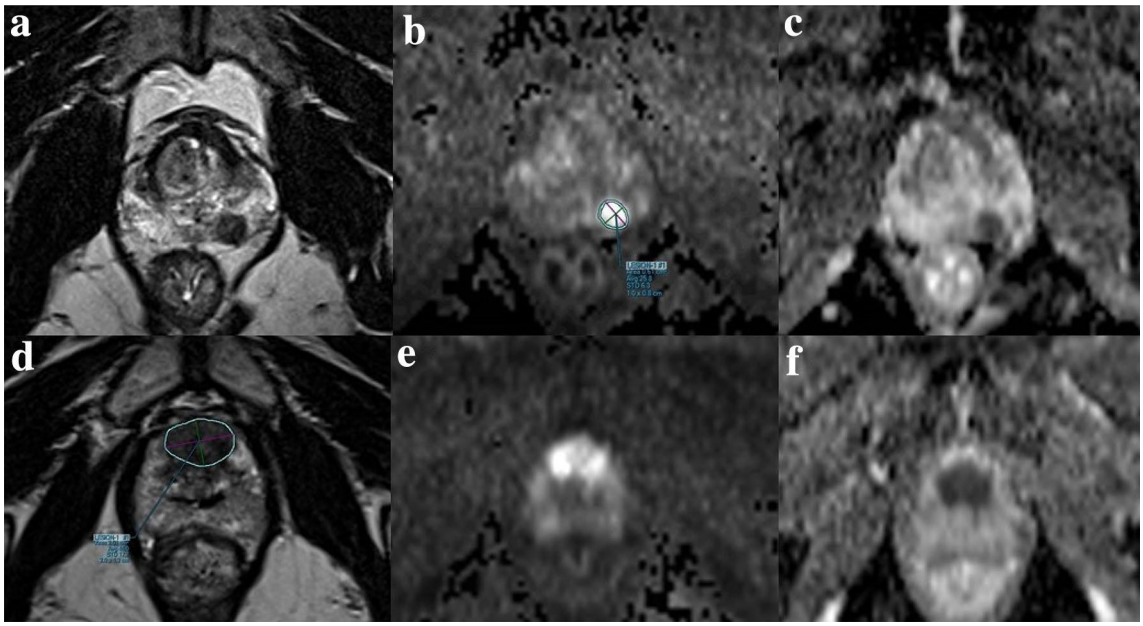


**Fig. 2.**

Prostate cancer in peripheral zone (PZ) in **a** T2-weighted MR image; **b** diffusion-weighted image (main sequence for lesion scoring and size measurement (1 cm) based on PI-RADSv2 criteria for PZ); **c** apparent diffusion coefficient (ADC) map; and in transition zone (TZ) in **d** T2-weighted MR image (main sequence for lesion scoring and size measurement (2 cm) based on PI-RADSv2 criteria for TZ); **e** diffusion-weighted image; **f** apparent diffusion coefficient (ADC) map

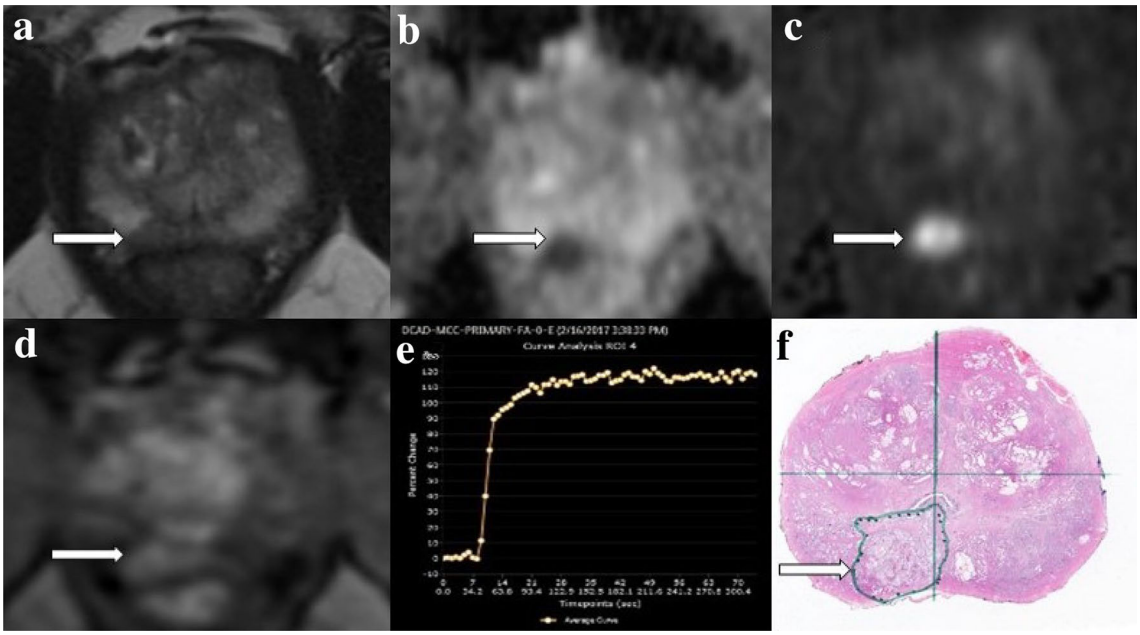


**Fig. 3.**

67-year-old man with PSA:11 ng/ml and a low-grade (Gleason score 3 + 3) true positive prostate cancer lesion (arrow) in the right posteromedial peripheral zone; **a** irregular mildly hypointense signal with irregular margins on axial T2-weighted MR image; **b** markedly hypointense on axial apparent diffusion coefficient (ADC) map (value 613); **c** focal markedly hyperintense on diffusion-weighted image; **d** focal, early and mildly intense enhancement on dynamic contrast-enhanced (DCE) MRI; **e** DCE enhancement curve (type 2); **f** whole mount histopathology cut at 4 μm and stained with Hematoxylin and Eosin

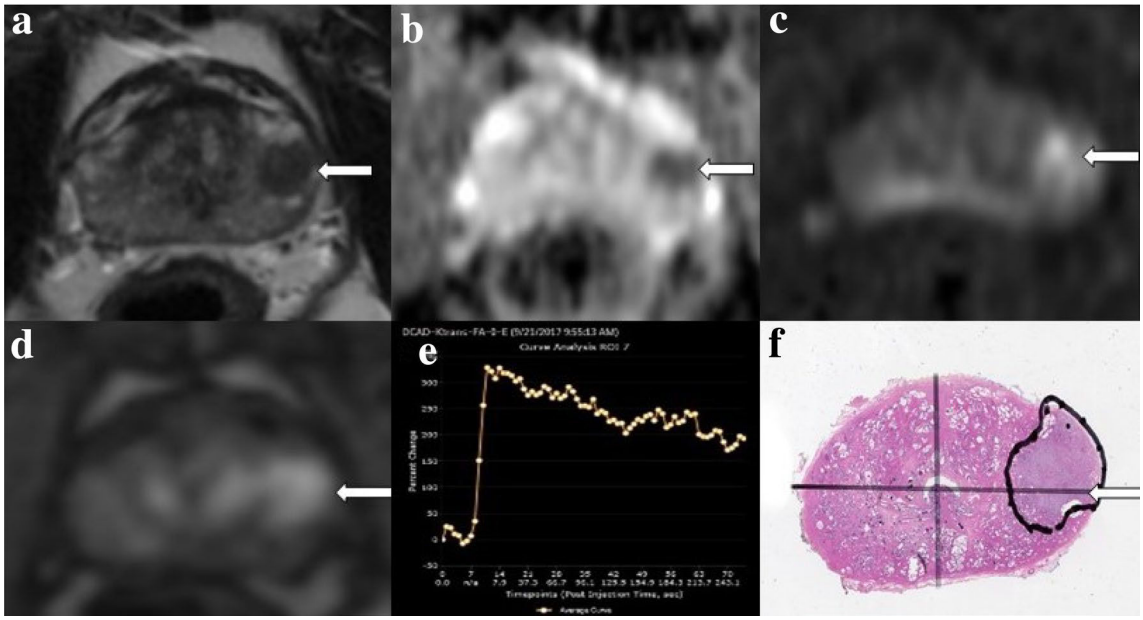


**Fig. 4.**

62-year-old man with PSA: 9.6 ng/ml and a high-grade (Gleason score 4 + 3) true positive prostate cancer lesion (arrow) in the left lateral peripheral zone; **a** round markedly hypointense signal with circumscribed margins on axial T2-weighted MR image; **b** maderately hypointense on axial apparent diffusion coefficient (ADC) map (value 733); **c** focal markedly hyperintense on Diffusion-weighted image; **d** focal, early and intense enhancement on dynamic contrast-enhanced (DCE) MRI; **e** DCE enhancement curve (type 3); **f** whole mount histopathology cut at 4 microns and stained with Hematoxylin and Eosin

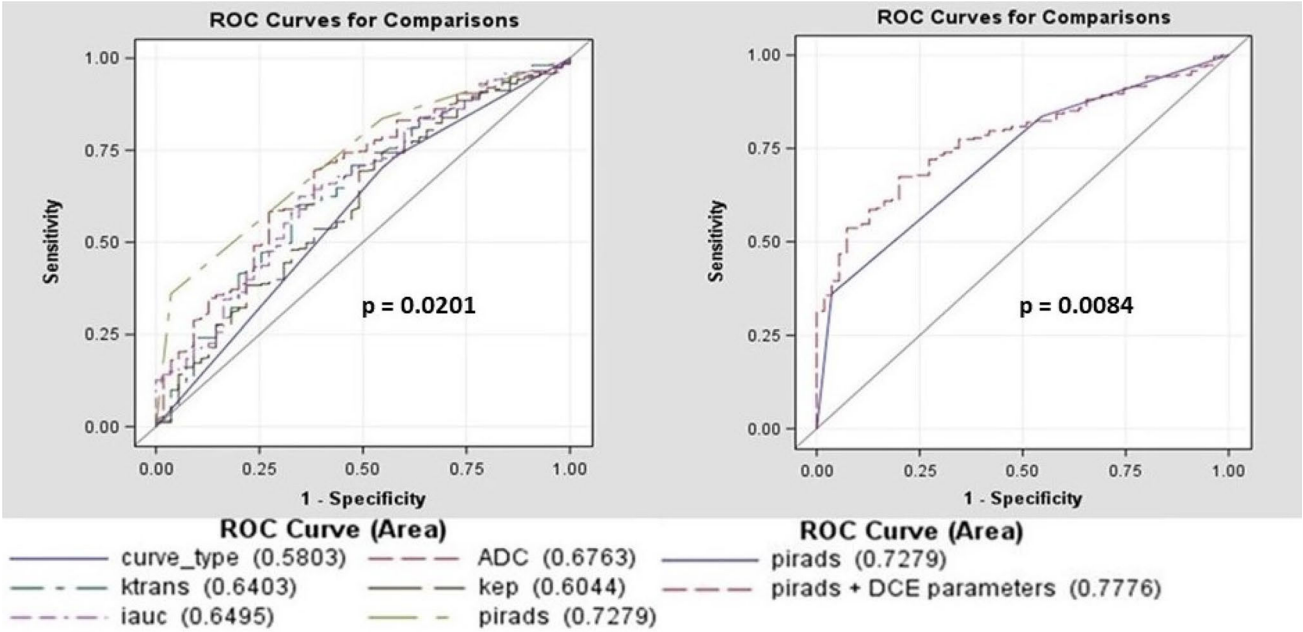


**Fig. 5.**

Comparison of prostate cancer tumor grading ROC curves a; for PI-RADSv2 category, Apparent Diffusion Coefficient (ADC) value and Dynamic contrast-enhanced (DCE) qualitative and quantitative parameters, individually and b; for Prostate Imaging–Reporting and Data System version 2 (PI-RADSv2) and combination of PI-RADSv2 and DCE qualitative and quantitative parameters (the *p* values are for the comparisons between all features in each ROC analysis)

**Table 1**

3T multiparametric MRI protocol for all scanners in the study (the ranges are provided)

| | TR/TE[a] (ms/ms) | Echo train length | FOV[b] (cm) | Matrix | Slice thickness (mm) |
|---|---|---|---|---|---|
| 2D axial T2WI[c] | 3800–5040/101 | 101 | 20×20 | 320×310 | 3 |
| DWI[d] echo-planar | 3300–4800/60–80 | 47 | 21×26 | 160×94 | 3.6 |
| DCE[e] | 3.85–4.23/1.42–1.52 | – | 26×26 | 160×160 | 3.6 |

[a] Repetition time/echo time

[b] Field of view

[c] T2-weighted imaging

[d] Diffusion-weighted imaging; The b values were 0, 100, 400, and 800 s/mm$^2$ with a calculated or natively acquired b value of 1400 s/mm2 and average Apparent Diffusion Coefficient (ADC) mapping of the most characteristic subarea of the tumor

[e] Dynamic contrast-enhanced

*Abdom Radiol (NY)*. Author manuscript; available in PMC 2023 June 13.

**Table 2**

Clinical, magnetic resonance imaging and pathology characteristics

| Variable | Value |
|---|---|
| Patient number | 254 |
| Age (mean ± SD) years | 62.1 ± 7.6 |
| PSA[a] (median) ng/ml | 6 (IQR 3.9) |
| PSA density (median) ng/ml/cc | 0.17 (IQR 0.11) |
| Endorectal coil | 56.7% (144/254) |
| Prostate volume (median) cc | 35 (IQR 16) |
| Lesion location | 323 |
| Transition zone | 72 (22.3%) |
| Peripheral zone | 251 (77.7%) |
| PI-RADSv2 | 323 |
| Category 3 | 106 (32.8%) |
| Category 4 | 120 (37.2%) |
| Category 5 | 97 (30%) |
| Pathology Gleason score | 323 |
| 3 + 3 | 57 (17.6%) |
| 3 + 4 | 164 (50.8) |
| 3 + 5 | 6 (1.9%) |
| 4 + 3 | 63 (19.5%) |
| 4 + 4 | 13 (4%) |
| 4 + 5 | 18 (5.6%) |
| 5 + 3 | 2 (0.6%) |
| Pathology stage | 323 |
| pT2a | 82 (25.4%) |
| pT2b | 16 (5%) |
| pT2c | 12 (3.7%) |
| pT3a | 95 (29.4%) |
| pT3b | 93 (28.8%) |
| pT4 | 25 (7.7%) |
| Prostate weight (median) g | 40 (IQR 19) |
| Pathology tumor size (median) cm | 2 (IQR 1.4) |

[a] prostate specific antigen

[b] Prostate Imaging–Reporting and Data System version 2

**Table 3**

Comparison of dynamic contrast-enhanced magnetic resonance imaging of qualitative and quantitative parameters in prostate cancer lesions based on tumor grading

| | Overall | Index | Peripheral | Transition | ≥ 1 cm | < 1 cm |
|---|---|---|---|---|---|---|
| $K^{trans}$ [median (Q1–Q3[a])] | $p = 0.005$ * | $p = 0.379$ | $p = 0.005$ * | $p = 0.650$ | $p = 0.035$ * | $p = 0.483$ |
| Low grade | 0.32 (0.21–0.52) | 0.37 (0.24–0.61) | 0.31 (0.21–0.46) | 0.35 (0.21–0.7) | 0.33 (0.22–0.61) | 0.31 (0.2–0.46) |
| High grade | 0.43 (0.29–0.69) | 0.42 (0.29–0.68) | 0.43 (0.29–0.71) | 0.4 (0.33–0.58) | 0.43 (0.29–0.69) | 0.23 (0.21–0.78) |
| $K_{ep}$ [median (Q1–Q3)] | $p = 0.081$ | $p = 0.466$ | $p = 0.220$ | $p = 0.490$ | $p = 0.100$ | $p = 0.375$ |
| Low grade | 1.31 (0.79–1.9) | 1.36 (0.79–2.14) | 1.38 (0.92–1.9) | 1.23 (0.64–1.65) | 1.27 (0.77–1.87) | 1.38 (0.83–1.89) |
| High grade | 1.54 (1.06–2.57) | 1.52 (1.05–2.32) | 1.57 (1.06–2.6) | 1.44 (1.14–2.12) | 1.54 (1.06–2.52) | 1.62 (0.77–4.54) |
| iAUC [median (Q1–Q3)] | $p < 0.001$ * | $p = 0.048$ * | $p < 0.001$ * | $p = 0.410$ | $p = 0.002$ * | $p = 0.640$ |
| Low grade | 6.9 (4.99–9.67) | 7.42 (4.98–10.63) | 6.67 (5.21–8.43) | 7.6 (4.54–12.53) | 6.9 (5.01–10.25) | 7.08 (4.64–8.75) |
| High grade | 8.99 (6.6–12.15) | 8.94 (6.63–12.14) | 9 (6.54–12.19) | 8.96 (7.32–11.36) | 9.06 (6.6–12.19) | 7.41 (5.55–10.98) |
| Curve type | $p = 0.044$ * | $p = 0.800$ | $p = 0.535$ | $p = 0.029$ * | $p = 0.280$ | $p = 0.130$ |
| Low grade | 57 | 22 | 34 | 23 | 35 | 22 |
| Type 1 | 2 (3.5%) | 0 (0%) | 1 (2.9%) | 1 (4.3%) | 2 (5.7%) | 0 (0%) |
| Type 2 | 24 (42.1%) | 7 (31.8%) | 12 (35.3%) | 12 (52.2%) | 12 (34.3%) | 12 (54.5%) |
| Type 3 | 31 (54.4%) | 15 (68.2) | 21 (61.8%) | 10 (43.5%) | 21 (60%) | 10 (45.5%) |
| High grade | 266 | 232 | 217 | 49 | 255 | 11 |
| Type 1 | 9 (3.4%) | 7 (3%) | 8 (3.7%) | 1 (2%) | 8 (3.1%) | 1 (9.1%) |
| Type 2 | 70 (26.3%) | 60 (25.9%) | 58 (26.7) | 12 (24.5%) | 67 (26.3%) | 3 (27.3%) |
| Type 3 | 187 (70.3%) | 165 (71.1%) | 151 (69.6%) | 36 (73.5%) | 180 (70.6%) | 7 (63.6%) |

The reported *p* values are for all the categories in each column

*Statistically significant

[a]Quartile 1–3

**Table 4**

Comparison of dynamic contrast-enhanced magnetic resonance imaging qualitative and quantitative parameters in prostate cancer lesions based on Prostate Imaging–Reporting and Data System version 2

| | Overall | Index | Peripheral | Transition | ≥ 1 cm | < 1 cm |
|---|---|---|---|---|---|---|
| $K^{trans}$ [median (Q1–Q3[a])] | $p < 0.001$ * | $p = 0.074$ | $p < 0.001$ * | $p = 0.645$ | $p < 0.001$ * | $p = 0.652$ |
| 3 | 0.34 (0.22–0.58) | 0.41 (0.21–0.58) | 0.32 (0.21–0.56) | 0.37 (0.24–0.7) | 0.34 (0.22–0.61) | 0.32 (0.22–0.51) |
| 4 | 0.39 (0.29–0.64) | 0.27 (0.29–0.63) | 0.4 (0.29–0.66) | 0.35 (0.29–0.52) | 0.4 (0.29–0.64) | 0.30 (0.16–0.51) |
| 5 | 0.51 (0.31–0.80) | 0.72 (0.32–0.81) | 0.53 (0.32–0.81) | 0.45 (0.3–0.8) | 0.52 (0.31–0.8) | 1.03[b] |
| $K_{ep}$ [median (Q1–Q3)] | $p = 0.004$ * | $p < 0.001$ * | $p = 0.002$ * | $p = 0.486$ | $p = 0.002$ * | $p = 0.577$ |
| 3 | 1.29 (0.79–2.06) | 1.17 (0.78–1.86) | 1.26 (0.78–2.06) | 1.33 (0.83–2.11) | 1.25 (0.8–1.92) | 1.36 (0.8–2.1) |
| 4 | 1.49 (1.08–2.28) | 1.51 (1.12–2.1) | 1.56 (1.12–2.53) | 1.22 (0.86–1.64) | 1.49 (1.12–2.2) | 1.58 (0.84–2.7) |
| 5 | 1.75 (1.19–2.98) | 1.79 (1.17–2.98) | 1.81 (1.17–3.13) | 1.67 (1.2–2.74) | 1.77 (1.17–2.98) | 4.54[b] |
| iAUC [median (Q1–Q3)] | $p = 0.002$ * | $p < 0.001$ * | $p = 0.001$ * | $p = 0.548$ | $p = 0.008$ * | $p = 0.770$ |
| 3 | 7.60 (5.12–10.7) | 8.45 (4.84–10.8) | 7.34 (5–10.15) | 8.34 (6.21–13.06) | 7.76 (5.12–11) | 7.2 (5.21–9.38) |
| 4 | 8.54 (6.52–11.35) | 7.10 (6.75–11.7) | 8.71 (6.4–11.7) | 7.83 (6.8–11.11) | 8.68 (6.55–11.47) | 6.8 (4.7–8.98) |
| 5 | 9.79 (7.21–12.9) | 11.3 (7.24–12.93) | 9.83 (7.02–12.93) | 9.74 (7.6–11.39) | 9.82 (7.02–12.93) | 10.98[b] |
| Curve type | $p < 0.001$ * | $p = 0.002$ * | $p = 0.003$ * | $p = 0.060$ | $p < 0.001$ * | $p = 0.350$ |
| 3 | 106 | 64 | 71 | 35 | 82 | 24 |
| Type 1 | 7 (6.6%) | 5 (7.8%) | 6 (8.5%) | 1 (2.9%) | 7 (8.5%) | 0 (0%) |
| Type 2 | 44 (41.5%) | 24 (37.5%) | 28 (39.4%) | 16 (45.7%) | 32 (39%) | 12 (50%) |
| Type 3 | 55 (51.9%) | 35 (54.7%) | 37 (52.1%) | 18 (51.4%) | 43 (52.4%) | 12 (50%) |
| 4 | 120 | 98 | 100 | 20 | 112 | 8 |
| Type 1 | 3 (2.5%) | 2 (2%) | 2 (2%) | 1 (5%) | 2 (1.8%) | 1 (12.5%) |
| Type 2 | 32 (26.7%) | 25 (25.5%) | 26 (26%) | 6 (30%) | 29 (25.9%) | 3 (37.5%) |
| Type 3 | 85 (70.8%) | 71 (72.5%) | 72 (72%) | 13 (65%) | 81 (72.3) | 4 (50%) |
| 5 | 97 | 92 | 80 | 17 | 96 | 1 |
| Type 1 | 1 (1%) | 0 (0%) | 1 (1.25%) | 0 (0%) | 1 (1%) | 0 (0%) |
| Type 2 | 18 (18.6%) | 18 (19.6%) | 16 (20%) | 2 (11.8%) | 18 (18.8%) | 0 (0%) |
| Type 3 | 78 (80.4%) | 74 (80.4%) | 63 (78.7%) | 15 (88.2%) | 77 (80.2%) | 1 (100%) |

The reported *p* values are for all the categories in each column

*Abdom Radiol (NY)*. Author manuscript; available in PMC 2023 June 13.

* Statistically significant

[a] Quartile 1–3

[b] only one lesion in this group